Soft Materials
Publication details, including instructions for authors and subscription information:
http://www.tandfonline.com/loi/lsfm20

Gel Ability and Fluorescence-Enhanced Emission of a New Bi-1,3,4-Oxadiazole Derivative

Chengxiao Zhao [a], Haitao Wang [a], Songnan Qu [b], Peng Zhang [a], Binglian Bai [c], Xia Ran [a], Huimin Liu [a], Yan Zhang [a] & Min Li [a]

[a] Key Laboratory for Automobile Materials, Ministry of Education, Institute of Materials Science and Engineering, Jilin University, Changchun, P. R. China

[b] Key Laboratory of Excited State Processes, Changchun Institute of Optics, Fine Mechanics and Physics, Chinese Academy of Sciences, Changchun, P. R. China

[c] College of Physics, Jilin University, Changchun, P. R. China

Published online: 22 Feb 2013.

Soft Materials (2013) **11**, 261–271

ISSN: 1539-445X print / 1539-4468 online
DOI: 10.1080/1539445X.2011.633147

Gel Ability and Fluorescence-Enhanced Emission of a New Bi-1,3,4-Oxadiazole Derivative

CHENGXIAO ZHAO[1], HAITAO WANG[1], SONGNAN QU[2], PENG ZHANG[1], BINGLIAN BAI[3], XIA RAN[1], HUIMIN LIU[1], YAN ZHANG[1], and MIN LI[1]*

[1]*Key Laboratory for Automobile Materials, Ministry of Education, Institute of Materials Science and Engineering, Jilin University, Changchun, P. R. China*
[2]*Key Laboratory of Excited State Processes, Changchun Institute of Optics, Fine Mechanics and Physics, Chinese Academy of Sciences, Changchun, P. R. China*
[3]*College of Physics, Jilin University, Changchun, P. R. China*

Received August 19, 2011, Accepted October 14, 2011

A new bi-1,3,4-oxadiazole derivative (BOXDH-T12) was synthesized. BOXDH-T12 shows very strong gelation ability in DMF and n-octanol with critical gelation concentrations of 1.1×10^{-3} and 6.0×10^{-4} mol/L, respectively, due to the intermolecular hydrogen bonding. X-ray diffractions of BOXDH-T12 xerogels from DMF and n-octanol showed different microstructures. Fluorescence enhanced emissions were observed during DMF gel formation of BOXDH-T12, which was attributed to J-aggregation. The emission band 500 nm of BOXDH-T12 in DMF solutions at 353 K is characterized by a strong excimer emission.

[Supplemental materials are available for this article. Go to the publisher's online edition of Soft Materials to view the free supplemental file: Supplemental Figures.]

Keywords: bi-1,3,4-oxadiazole, excimer, fluorescence, J-aggregation, organogel

Introduction

Organogels, in which organic solvents are gelled by low-molecular-weight compounds (organogelators), have attracted much interest as a result of their unique features and potential applications for new organic soft materials (1–3). These organogelators create a three-dimensional network by self-organization through noncovalent interactions such as hydrogen bonds (4, 5), hydrophobic interaction (6), π-π interaction (7), van der Waals force (8–11), electron donor-acceptor interaction (12, 13), and so forth. Therefore, gel ability is always related to the noncovalent interactions. However, hydrogen bonding is more meaningful to gel stability due to its directionality and strength. In this context, we will improve the gel ability by introducing hydrogen bonding.

A gelator molecule containing well-established fluorophores has attracted considerable attention over recent years due to its prospective application in drug delivery and release (14, 15), photo-responsive materials (16), sensors for chemical surroundings (17, 18), organic light-emitting diodes (OLEDs) (19, 20), and so on. Because organogels are formed through self-assembly of low-molecular-mass organogelators, a fluorescent gelator might exhibit significant fluorescence emission in gel, for example, fluorescence enhanced or quenched emissions (21–23). The fluorescence enhanced emissions of gels were unambiguously assigned to the phenomenon of aggregation-induced emission (AIE) (24–26), which was attributed to the restricted intramolecular rotational motions and J-aggregate formation (27–29).

Recently, we reported that bi-1,3,4-oxadiazole derivatives (BOXD-Tn) exhibited good emission properties and gelation ability (12, 13); especially, BOXD-T8 showed prominent gelation ability and enhanced emission (J-aggregation) in ethanol. Investigations have revealed that intermolecular electron donor-acceptor interaction (12, 13, 28) is the main driving force for gelation, and the coplanar conformation of 2,2'-bi-phenyl-bi-1,3,4-oxadiazole and J-aggregation are the reasons for the strong fluorescence emission. We also have reported a series of hydrazine derivatives (BPH-n) that were super gelators due to intermolecular hydrogen bonding (29). In the present paper, we report the synthesis, gelation, and fluorescence properties of a new bi-1,3,4-oxadiazole derivative (BOXDH-T12) that contains amide groups (hydrogen bonding group) and a 2,2'-bi-phenyl-bi-1,3,4-oxadiazole rigid core (well-established fluorophore). The present molecular design aimed at introducing lateral intermolecular hydrogen bonding to adjust its gel ability and fluorescence properties. It was demonstrated that BOXDH-T12 behaves as a

*Address correspondence to: Min Li, Key Laboratory for Automobile Materials, Ministry of Education, Institute of Materials Science and Engineering, Jilin University, Changchun 130012, P. R. China. Email: minli@mail.jlu.edu.cn

super gelator in DMF and n-octanol, its xerogels, shows different morphologies (ribbons, fibers). During the DMF gel formation, enhanced emission was detected.

Results and Discussions

Gelation Properties

The gels were prepared by mixing a weighed sample with solvent in a sealed test tube and heating the mixture until the solid dissolved and then held at room temperature for 30 min. The gelling properties of BOXDH-T12 in different solvents are summarized in Table 1. BOXDH-T12 can be dissolved in chloroform easily; precipitated from acetone, ethanol, and toluene; and gel DMF and n-octanol with the critical gelation concentrations (CGCs) of 1.2×10^{-3} and 6.0×10^{-4} mol/L, respectively. The low CGC values suggest that BOXDH-T12 behaves as a super gelator in DMF and n-octanol (30, 31). Figure 1 shows gel-sol phase-transition temperatures (T_{gel}s) of DMF and n-octanol gels of BOXDH-T12 as a function of concentration (T_{gel}s values were measured through the "falling drop" method (32)). The T_{gel} value of DMF gel increases from 293 K at 1.2×10^{-3} mol/L to 326 K at 3.7×10^{-3} mol/L, and the T_{gel} of n-octanol gel increases from 293 K at 6.0×10^{-4} mol/L to 351 K at 3.2×10^{-3} mol/L. Both gels could repeat the gel-sol transition process many times, and they could be stably held at room temperature.

In order to evaluate the driving forces for gelation of BOXDH-T12, we measured the FT-IR spectra. Figure 2 shows the FT-IR spectra of BOXDH-T12 film coated from chloroform and the xerogel from DMF. The typical absorption bands of C=O were observed around 1680, 1657, and 1649 cm^{-1} in both spectra indicating intermolecular hydrogen bonding participated in forming supramolecules (33, 34). The absorption bands arising from the antisymmetric ($\nu_{as}CH_2$) and symmetric (ν_sCH_2) stretching vibrations of alkyl chains were observed at 2925 and 2853 cm^{-1} in the film from chloroform (Fig. 2a), suggesting the presence of a gauche form alkyl chain. These IR bands appeared at 2918 ($\nu_{as}CH_2$) and 2848 cm^{-1} (ν_sCH_2) in the xerogel from DMF, corresponding to the alkyl chain of the all-trans form. Consequently, it is clear that the van der Waals interaction between the alkyl chains is strong in DMF gel. On the other hand, the IR bands of 1598 cm^{-1} assigned to phenyl rings in the film from chloroform shifted to 1590 cm^{-1} in the xerogel from DMF, revealing stronger π-π interaction in DMF gel. Furthermore, ^1H NMR diluting experiments of BOXDH-T12 were carried out in $CDCl_3$ at room temperature (Fig. 3). Concentration-dependent ^1H NMR spectra show that increasing concentrations of BOXDH-T12 in $CDCl_3$ from 0.05 to 20 mM caused remarkable broadening and downfield shift of N-H from 7.89 ppm (non-association) to 8.07 ppm

Table 1. Gelation properties of BOXDH-T12 in different solvents.[a]

	DMF	Acetone	Ethanol	Chlorlform	Toluene	n-octanol
BOXDH-T12	1.2×10^{-3}	P	P	S	P	6.0×10^{-4}
BBOXD-T10	P	P	P	S	S	6.7×10^{-3}

S, soluble; P, precipitation.
[a]Values denote the minimum gel concentration (mol/L) necessary for organogelation.

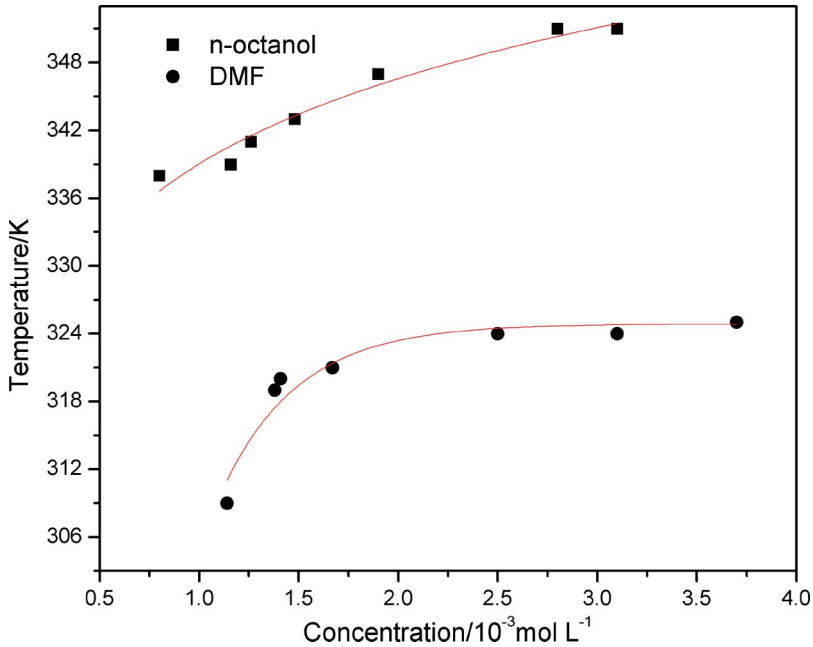

Fig. 1. Concentration-dependent gel-sol phase-transition temperatures of BOXDH-T12 gels in DMF and n-octanol (color figure available online).

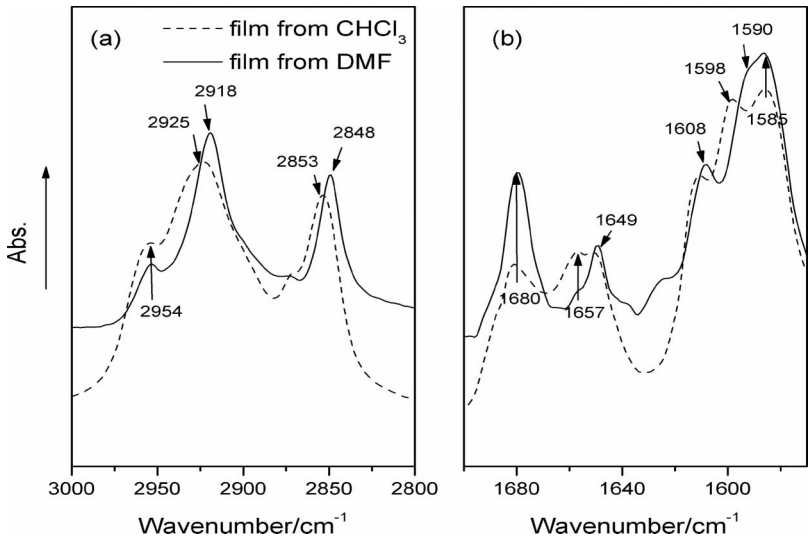

Fig. 2. FT-IR spectra of BOXDH-T12 films from $CHCl_3$ and DMF.

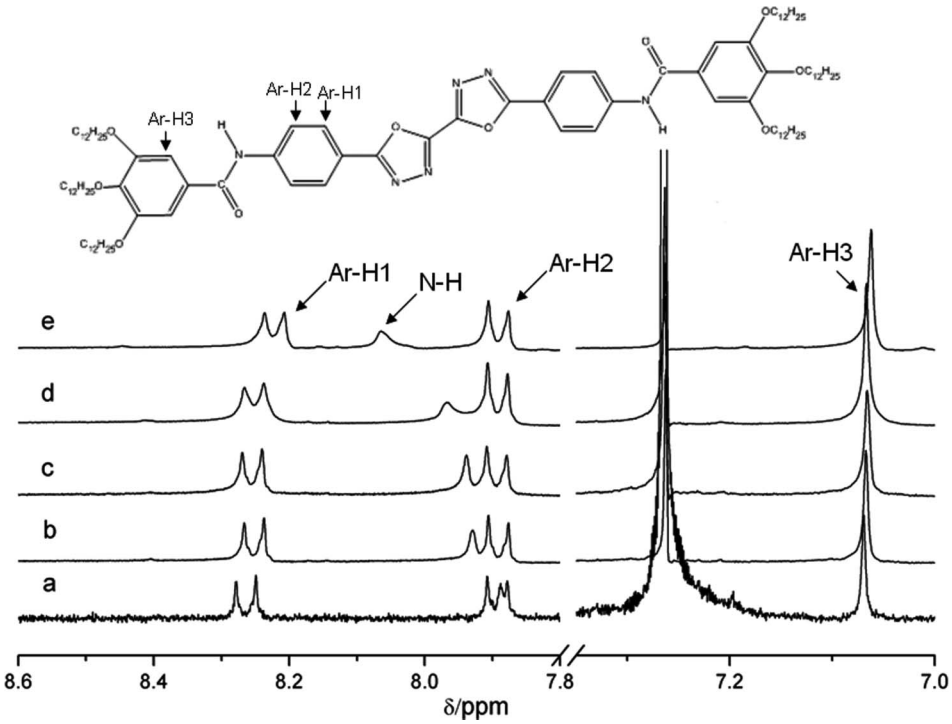

Fig. 3. Partial ^{1}H NMR spectra (300MHz, CDCl3, 298 K) of BOXDH-T12 at different concentrations. (a: 0.05 mM; b: 3.7 mM; c: 5.3 mM; d: 9.0 mM; e: 20 mM).

(self-association), suggesting hydrogen bonding between amide groups participated in forming supramolecules at high concentrations. Whereas, slightly upfield shifts for Ar-H1 (8.25 ppm, $\Delta\delta \approx 0.04$ ppm) and Ar-H3 (7.07 ppm, $\Delta\delta \approx 0.01$ ppm) were observed, indicating weak π-π interaction between neighboring phenyl rings.

The FT-IR spectra of the xerogels that form DMF and n-octanol are shown in Fig. 4. The BOXDH-T12 xerogel from n-octanol exhibits the N-H stretching vibration at around 3278 cm^{-1} and amide I vibration bands at 1651 cm^{-1}, which imply that the N-H groups are associated with C=O groups via N-H . . . O=C hydrogen bonding (33, 34). The N-H stretching vibration of the xerogel from DMF locates at 3325 cm^{-1} and amide I at 1680 and 1651cm^{-1}, which is similar to that at high temperatures (Fig. 1S, available online), and indicates weak hydrogen bonding formation, which may result from hydrogen bonding interactions between C=O of DMF and NH of amides (35).

Morphologies and Structures

In order to investigate the aggregation morphology of the gels, the xerogels from DMF and n-octanol were prepared and

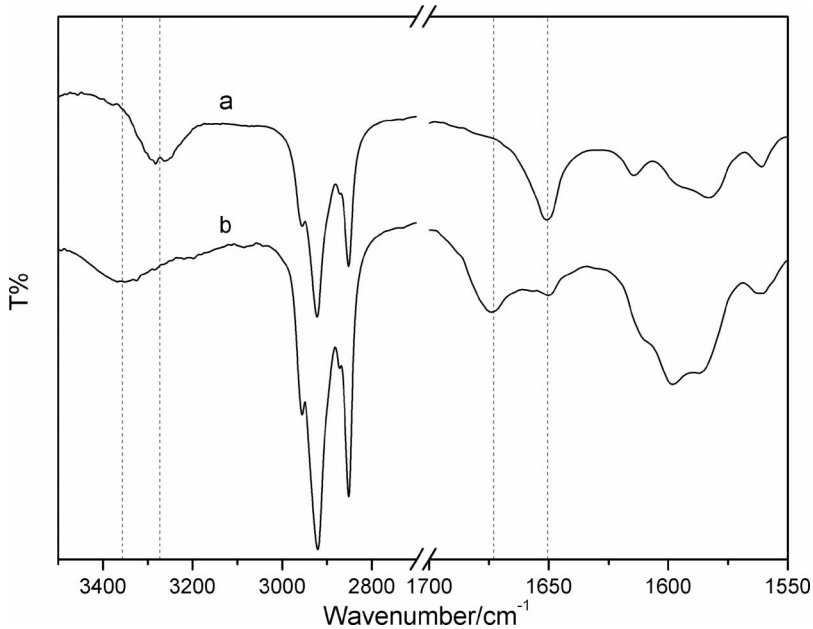

Fig. 4. FT-IR spectra of BOXDH-T12 xerogels from (a) DMF and (b) n-octanol.

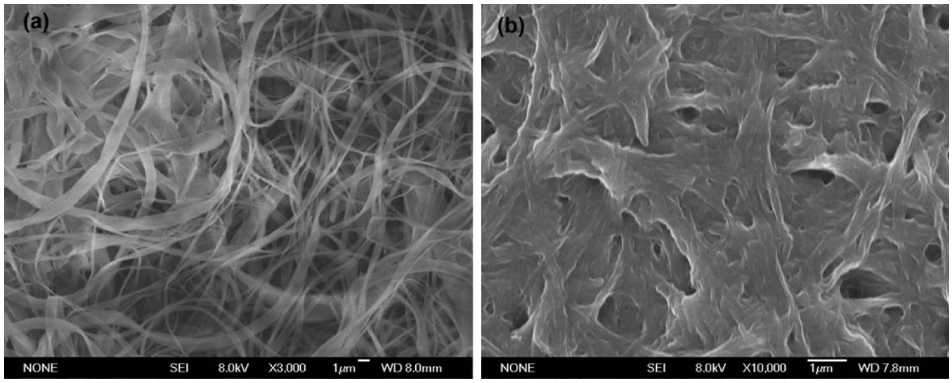

Fig. 5. FE-SEM images of BOXDH-T12 xerogels from (a) DMF and (b) n-octanol.

subjected to the scanning electron microscope (SEM) observation. As shown in Fig. 5a, the FE-SEM image of BOXDH-T12 xerogel from DMF consists of bundles of flexible ribbons within a width of 0.5–1 μm, while xerogel from n-octanol reveals a network structure composed of intertwined fibers within width of 0.4–1 μm (Fig. 5b). The formation of elongated ribbon-like or fiber aggregates implied that self-assembly of BOXDH-T12 was driven by strong directional intermolecular interactions. Figure 6 shows the XRD patterns of BOXDH-T12 xerogels from DMF and n-octanol. The xerogel from DMF exhibited one strong peak (49.5 Å) and four weak peaks (24.3, 12.1, 10.6, 9.3, 8.1 Å) in a low-angle range corresponding to a tetragonal columnar arrangement. Several weak peaks in the high-angle range suggested its crystalline feature (Fig. 6a), while the peak at 4.8 Å might be attributed to the repeated distance of bi-1,3,4-oxadiazole units in stacking. However, the xerogel from n-octanol showed a tetragonal columnar structure, which is different from the xerogel from DMF due to a strong peak (41.5 Å) and three weak peaks (20.7, 12.9, 8.3 Å) present in the low-angle range.

Aggregation-Induced Enhanced Emission

Interestingly, enhanced fluorescence emission was observed in DMF gel of BOXDH-T12, as shown in Fig. 7, the fluorescence intensity of DMF gel was about 100-fold than in its isotropic solution. Moreover, the fluorescence efficiency (Φ_F) of the xerogel was 12%, which is higher than its dilute solution ($\Phi_F = 3\%$). Figure 8 shows different fluorescence lifetime decay profiles of the xerogel from DMF at the emission wavelengths of 428, 454, and 484 nm, and the mean lifetimes are 2.23, 3.92, and 5.37 ns (Table 2) respectively, which reveal that more than one emitting spices coexist in DMF gel.

In order to understand the emitting spices in DMF gel of BOXDH-T12, detailed concentration-dependent luminescence spectroscopy of BOXDH-T12 in DMF was performed. Significant changes were observed in concentration-dependent emission spectra at 353 K (Fig. 9). The emission peak kept constant at 412 nm with concentration increasing from 1.21×10^{-6} to 1.10×10^{-5} mol/L, indicating its monomeric feature. Whereas, upon concentrating from 1.1×10^{-5} to 1.2×10^{-3}

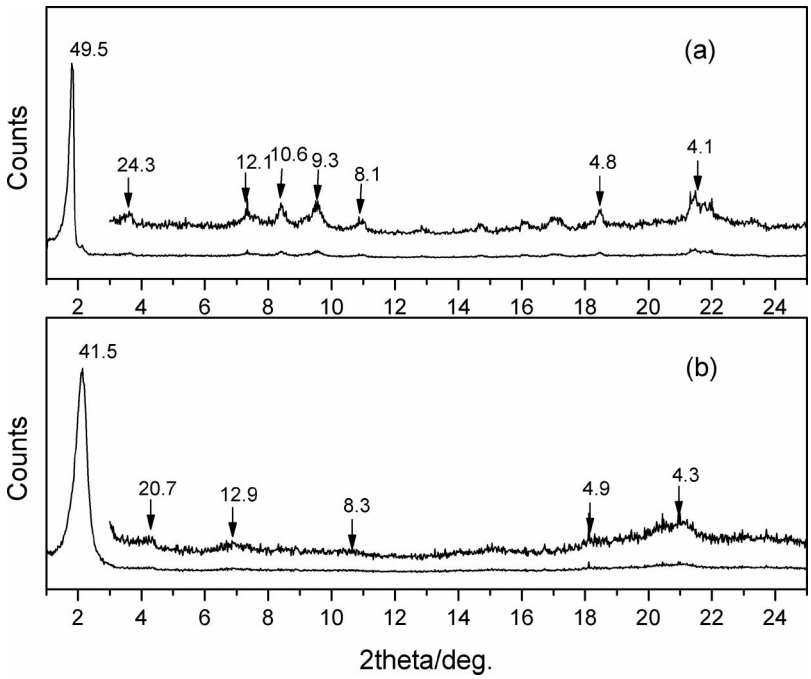

Fig. 6. X-ray diffraction patterns of BOXDH-T12 xerogels from (a) DMF and (b) n-octanol.

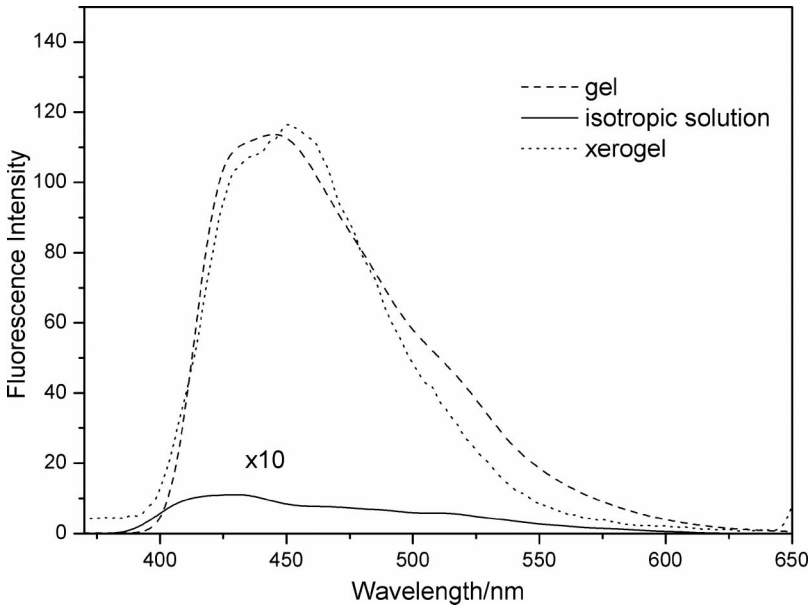

Fig. 7. Fluorescence spectra of isotropic solution (1.5×10^{-3} mol/L), gel and xerogel of BOXDH-T12.

mol/L, the emission at 412 nm shifted to 445 nm suggesting aggregation. The intensified obviously long wavelength of 500 nm that was similar to the emission of excimers.

To demonstrate the 412 nm emission band shifted to 445 nm with concentration increasing caused by aggregation, concentration-dependent excitation spectra of BOXDH-T12 in DMF were measured at emission band of 412–445 nm (Fig. 10). At a lower concentration (1.0×10^{-6} mol/L), the excitation spectrum showed a main peak at around 340 nm, which well-reserved the shape of the absorption spectrum. Significant broadening of the excitation peak was observed upon concentrating and the broad peak split into two new ones at 312 and 354 nm, respectively. The peak at 312 nm blue-shifted is attributed to H-aggregates, while the peak at 354 nm red-shifted comes from J-aggregates (36).

The emission band of 500 nm may be due to the excimer emission. First, one must be cautious that "excimer" emission might originate from a classic excimer that forms in and exists only in the excited state or related species that looks like an excimer but are preassociated BOXDH-T12 prior to optical excitation (excimer-like species) (37). To distinguish whether this band is due to ground-state species or not, excitation spectra

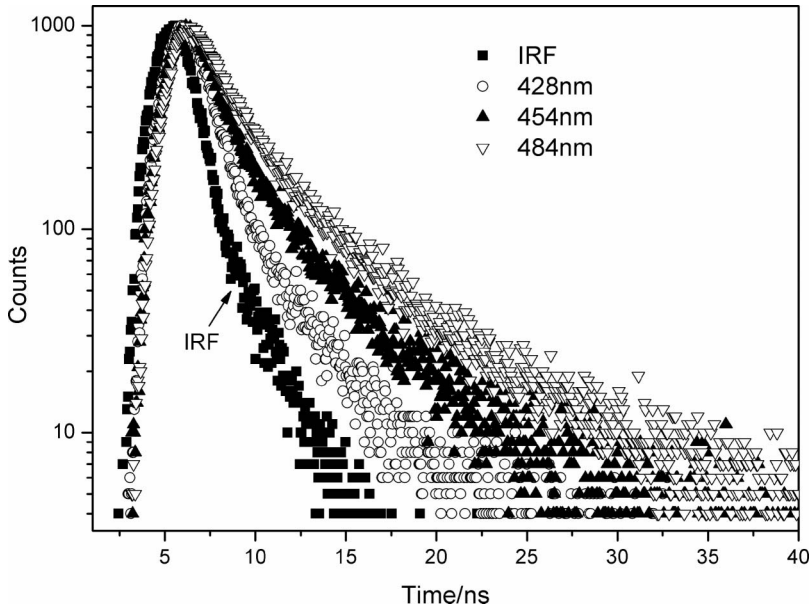

Fig. 8. Fluorescence lifetime decay profiles ($\lambda_{ex} = 340$ nm) of BOXDH-T12 xerogel from DMF monitored at different emission wavelengths. IRF = instrument response function.

Table 2. Fluorescence and fluorescence lifetime characteristics of BOXDT12 xerogels from DMF.

	λ_{em} [nm]	τ_1 [ns] (α_1)	τ_2 [ns] (α_2)	$<\tau>$ [ns]	χ^2
Xerogel from DMF	428	0.59 (88%)	4.15 (12%)	2.33	1.19
	454	0.92 (73%)	5.32 (27%)	3.92	1.13
	484	1.41 (64%)	6.83 (36%)	5.37	1.06

$\chi 2$, fitting parameter; τ_1 [ns], τ_2 [ns], fluorescence lifetime in nanoseconds; $<\tau>$ [ns], mean (average) fluorescence lifetime for biexponential decays, $\langle\tau\rangle = \frac{\alpha_1\tau_1^2+\alpha_2\tau_2^2}{\alpha_1\tau_1+\alpha_2\tau_2}$.

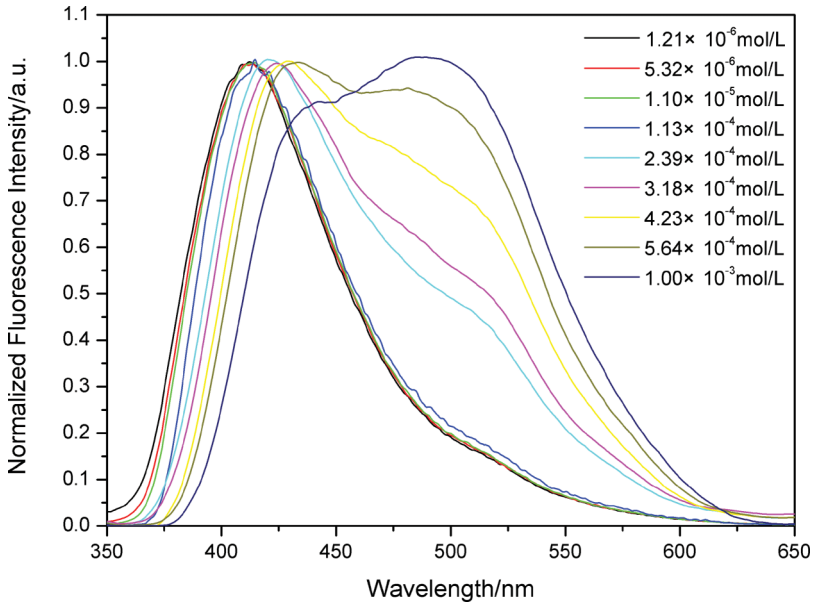

Fig. 9. Concentration-dependent fluorescence emission spectra of BOXDH-T12 in DMF at 353 K (color figure available online).

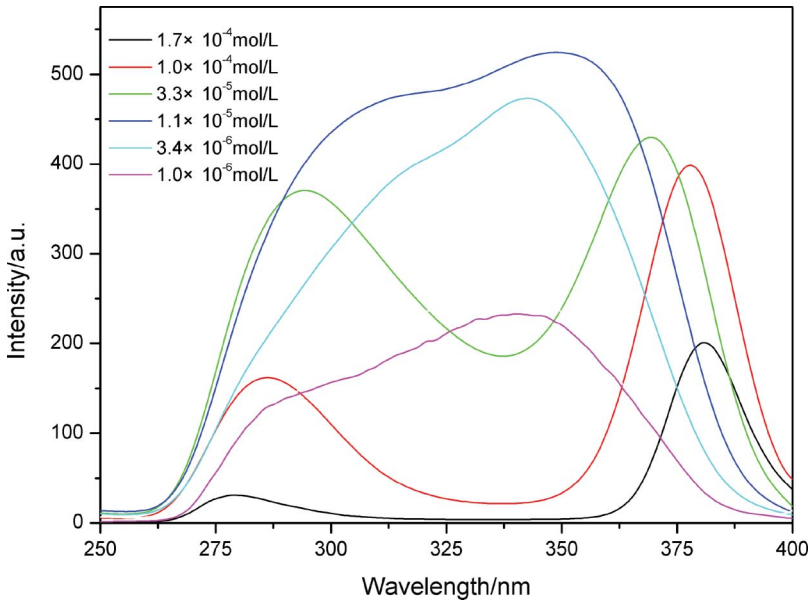

Fig. 10. Concentration-dependent excitation spectra for BOXDH-T12 in DMF recorded while monitoring the emission at 412 nm at 353 K (color figure available online).

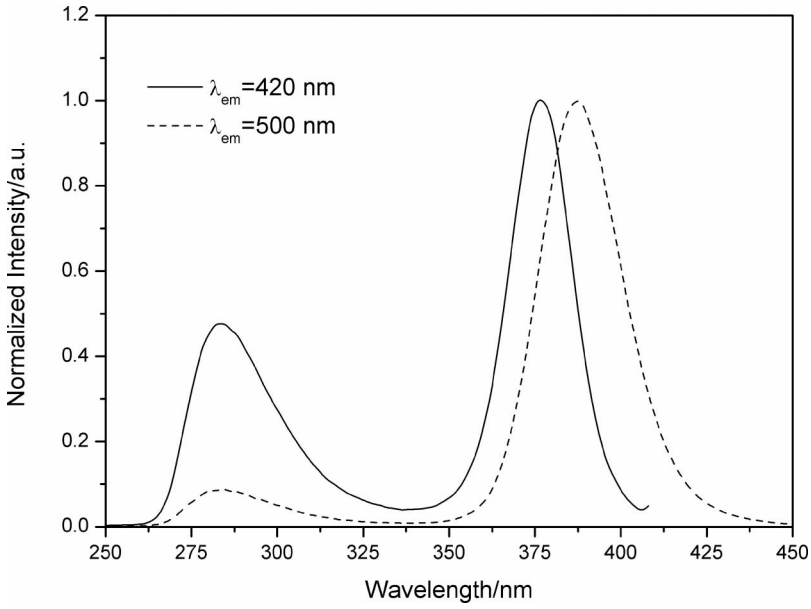

Fig. 11. Normalized emission wavelength-dependent excitation spectra for BOXDH-T12 in DMF recorded while monitoring the emission at 420 and 500 nm at 353 K. (Concentration = 2.3×10^{-4} mol/L).

of DMF solution of BOXDH-T12 at concentration of 2.3×10^{-4} mol/L were recorded upon observation at 420 and 500 nm (Fig. 11). The recognized emission-wavelength-dependent excitation spectra imply that the emission bands of 420 and 500 nm originated from different emitting species (38, 39). Emission at 500 nm was not observed in THF solution (Fig. 2S, available online) or in the mixture solvents of THF and DMF (Fig. 3S, available online), suggesting that the emission at 500 nm is not attributed to exciplexes or associated species between DMF and BOXDH-T12. The changes in I_E/I_M observed as a function of excitation wavelength are shown in Fig. 12. Exciting the DMF solution (1×10^{-4} mol/L) of BOXDH-T12 at 335, 350, 370, 375, 380, 385, and 390 nm led to incremental enhancement of I_E/I_M, and the position of the excimer band was not affected. Therefore, as stated previously, the likely cause of the emission of 500 nm intensification could be attributed to excimer-like species formation.

For further investigation of emitting spices in DMF gel, the temperature-dependent UV-vis and fluorescence spectra of BOXDH-T12 in high concentration DMF solutions were measured. As the temperature slowly decreased, the maximum emission of BOXDH-T12 in DMF solution (8×10^{-4} mol/L)

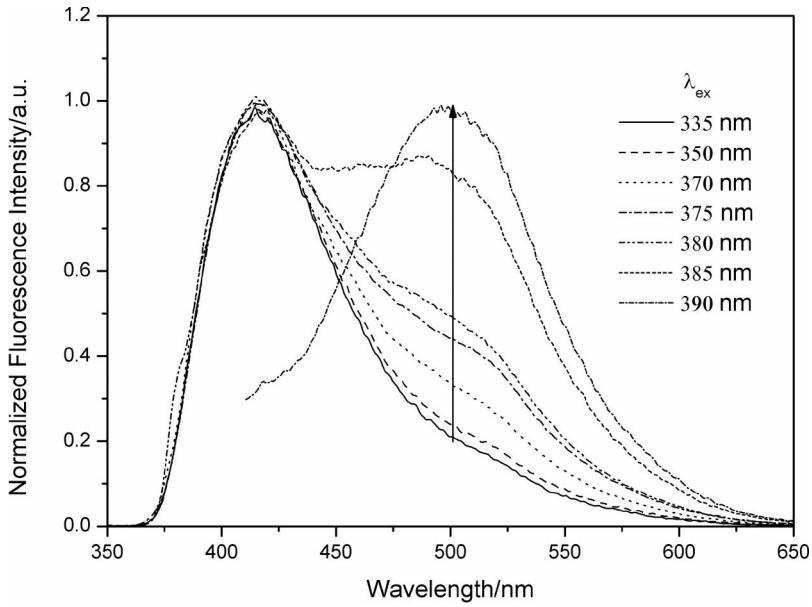

Fig. 12. Normalized fluorescence spectra of BOXDH-T12 in DMF solution at concentration of 1×10^{-4} mol/L with various excitation wavelengths.

significantly blue-shifted suddenly at 303 K (Fig. 4S, available online). Figure 13 shows the fluorescence and absorption spectra of BOXDH-T12 in DMF at 303 K with time aging. Not only were the blue-shifts of maximum emission and the excimer-like band observed but also the enhanced emission was detected (Fig. 13a). Simultaneously, the main absorption peak decreased observably and red-shifted slightly, while a new shoulder at around 395 nm intensified with time aging, indicating a J-aggregation feature (Fig. 13b) (40). J-aggregates can be demonstrated in a low concentration DMF solution of BOXDH-T12 at a lower temperature as well (Fig. 5S, available online).

Discussion

Considering twin-tapered BOXDH-T12 molecules, self-assembly of the BOXDH-T12 molecules through hydrogen bonding would cause the approach of neighboring molecules and induce π-π interactions between phenyl rings, which were confirmed by the ^{1}H NMR diluting experiment. However, hydrogen bonding interactions between DMF and BOXDH-T12 would cause the neighboring BOXDH-T12 molecules to slip along molecular axes and make the hydrogen bonding between BOXDH-T12 weak, which were evidenced by the X-ray diffraction pattern and FTIR spectrum of the xerogel from DMF. The first diffraction peak with d-spacing of 49.5 Å is close to the molecular length of BOXDH-T12 (52.6 Å). Upon all of the aforementioned, a J-aggregation packing model of BOXDH-T12 in DMF gel was proposed as shown in Fig. 14.

Experimental

General Methods

FT-IR spectra were recorded with a Perkin-Elmer spectrometer (Spectrum One B). The samples were pressed tablets with KBr. ^{1}H NMR spectra were recorded with a Varian-Unity 500MHz or VARIAN 300 MHz spectrometer, using tetramethylsilane (TMS) as an internal standard. ^{13}C NMR spectra were recorded with a VARIAN 300 MHz spectrometer, using chloroform-d as solvent and CDCl3 as an internal standard (δ =77.00ppm). Mass spectra were obtained by MALDI-TOF mass spectrometry. SEM observations were taken with a JSM-6700F apparatus or a SSX-550 apparatus. Photoluminescence was measured on a Perkin-Elmer LS 55 spectrometer and the absorption measurements were performed with a UV-2550 spectrometer. Fluorescence lifetimes were measured using an FL920 time-corrected single photon counting (TCSPC) system.

Synthesis and Characterizations

The N,N'-(4,4'-(2,2'-bi(1,3,4-oxadiazole)-5,5'-diyl)bis(4,1-phenylene))bis(3,4,5-tris(dodecyloxy)benzamide) (BOXDH-T12) is outlined in Scheme 1. The 5,5'-bis(4-nitrophenyl)-2,2'-bi(1,3,4-oxadiazole) was prepared according to previous literature (41). The 4.8-mmol compound 1 was suspended in 150 mL boiling ethanol and 0.16 mol sodium hydrogen sulfide (NaHS) in 30 mL water which was added within 20 min (42). After 30 min, the solids were filtered off and washed twice with water and hot ethanol, respectively, to give 5,5'-di(4-aminophenyl)-2,2'-bi(1,3,4-oxadiazole). According to the literature (43), 3,4,5-tri(dodecyloxy)benzoic acid could be obtained from the hydrolysis of the synthesized ethyl 3,4,5-tris(dodecyloxy)benzoate (44). The 2.2-mmol 3,4,5-tri(dodecyloxy)benzoic acid was converted to corresponding benzoic chloride (45). Then, it was regularly injected into 100 mL N-methylpyrrolidone (NMP) solution of compound 2 (1.1 mmol) and vigorously stirred at room temperature for 10 h; then, the solution was poured into 500 mL distilled water. The solids were filtered off and washed with water and hot ethanol. The crude dried product was dissolved into THF, filtered out of insoluble matters, and then the THF

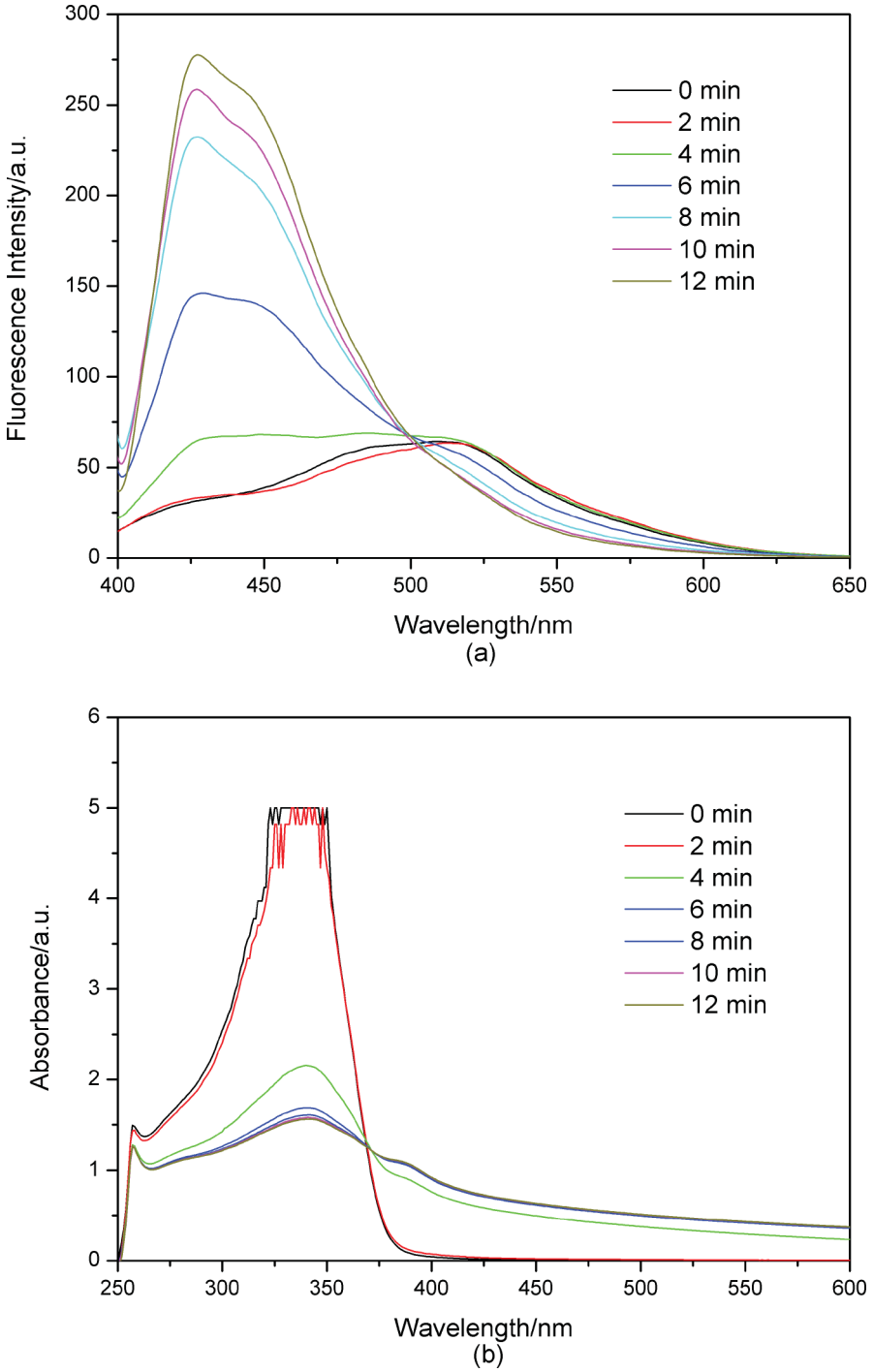

Fig. 13. (a) Absorption and (b) Fluorescence spectra (in a 0.1-cm cell) of BOXDH-T12 in DMF at 303 K with time aging. (Concentration $= 9 \times 10^{-4}$mol/L, $\lambda_{ex} = 390$ nm) (color figure available online).

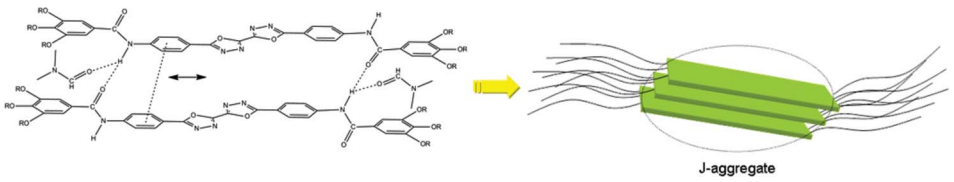

Fig. 14. J-aggregation packing mode for BOXDH-T12 gel in DMF (color figure available online).

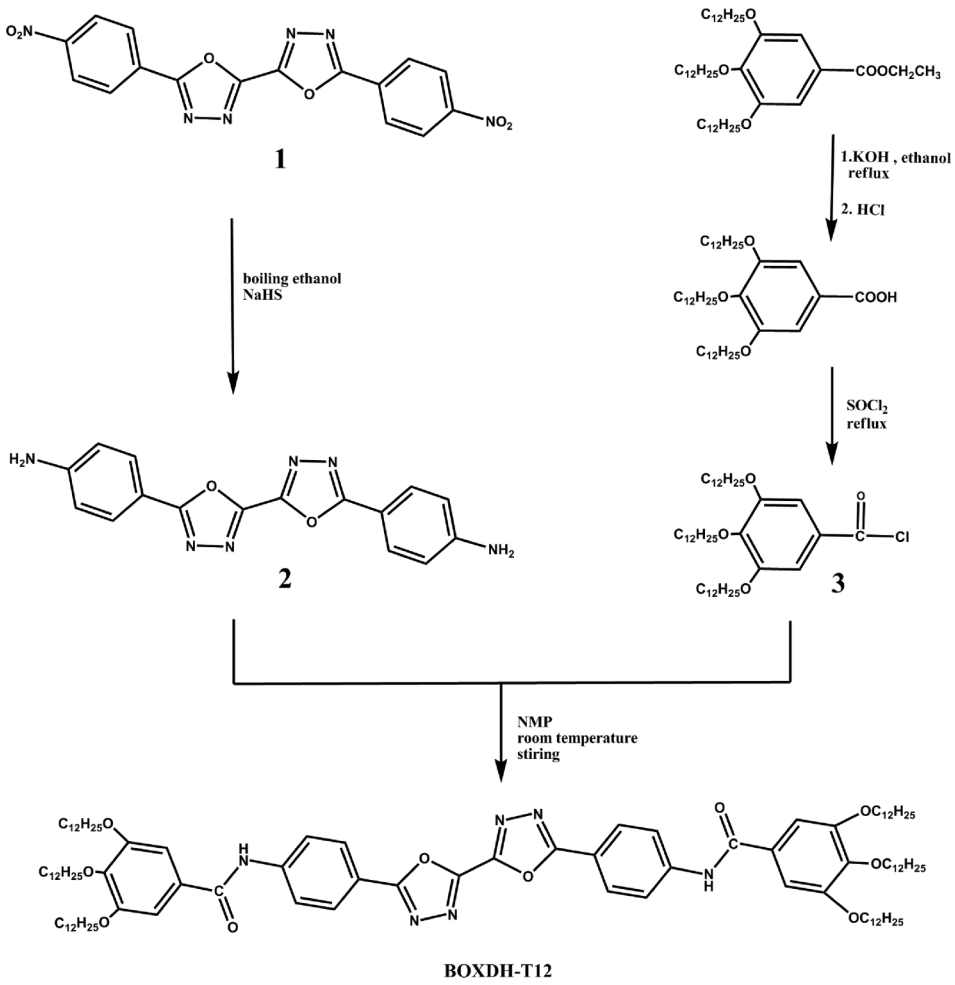

Scheme 1. Synthetic route of BOXDH-T12.

solvent was removed by a water bath and recrystallized from acetone/chloroform (volume ratio of 2:1) two times to obtain pure compound BOXDH-T12.

N,N'-(4,4'-(2,2'-bi(1,3,4-oxadiazole)-5,5'-diyl)bis(4,1-phenylene))bis(3,4,5-tris(dodecyloxy)benzamide).^{1}H NMR (300 MHz, $CDCl_3$,TMS): δ ppm 8.24–8.26 (d, J = 8.67Hz, 4H), 7.93(s, 2H), 7.90–7.88 (d, J = 8.75Hz, 4H), 7.07 (s, 4H), 4.02–4.06(q, J = 6.79Hz, 12H), 1.81–1.86 (m, 8H), 1.73–1.79 (m, 4H), 1.56 (s, 6H), 1.46–1.52 (m, 12H), 1.27–1.36 (m, 90H), 0.88–0.90 (t, J = 6.89Hz, 18H).

^{13}C NMR (300MHz, $CDCl_3$): δ ppm 165.9, 153.4, 152.8, 142.2, 129.1, 128.9, 120.1, 117.9, 105.9, 73.6, 69.5, 31.9, 30.3, 29.8,29.7, 29.6, 29.5, 29.4, 29.3, 26.1, 22.7, 14.1,

FT-IR: ν = 3291, 2955, 2922, 2870, 2852, 1650, 1612, 1593, 1583, 1560, 1521, 1500, 1467, 1428, 1411, 1385, 1339, 1245, 1214, 1183, 1163, 1119, 1080, 1048, 1020, 951, 858, 845, 831, 738, 720.

Anal. Calcd (%) for $C_{102}H_{164}N_6O_{10}$: C, 74.96; H, 10.11; N, 5.14. Found: C, 74.71; H, 10.39; N, 5.29.

MALDI-TOF MS: m/z: calcd for: 1635.3, found: 1635.1.

Conclusion

A novel oxadiazole derivative and BOXDH-T12 was synthesized and has been demonstrated to show gelation property in DMF, n-Octanol. BOXDH-T12 shows very low CGCs of 1.2 $\times 10^{-3}$ and 6.0 $\times 10^{-4}$ mol/L in DMF and n-octanol, respectively, due to the intermolecular hydrogen bonding. Excimer emissions and aggregation-induced enhanced emissions were observed in DMF, and the aggregation-induced enhanced emissions were attributed to J-aggregation, which phenomenon was confirmed via concentration- and temperature-dependent UV-vis and fluorescence spectroscopy.

Acknowledgments

The authors are grateful to the National Science Foundation Committee of China (Project No. 50873044, 51073071, and 21072076), and Project 985-Automotive Engineering of Jilin University for their financial support of this work.

References

1. Suzuki, M., Nakajima, Y., Yumoto, M., Kimura, M., Shirai, H., and Hanabusa, K. (2003) *Langmuir*, 19:8622–8624.
2. Terech, P., and Weiss, R. G. (1997) *Chem. Rev*., 97:3133–3160.
3. van Esch, J. H., and Feringa, B. L. (2000) *Angew. Chem., Int. Ed*., 39:2263–2266.
4. Suzuki, M., Saito, H., Shirai, H., and Hanabusa, K. (2007) *New J. Chem*., 31:1654–1660.
5. Qu, S. N., Wang, H. T., Yu, Z. X., Bai, B. L., and Li, M. (2008) *New J. Chem.*, 32:2023–2026.
6. Desvergne, J. P., Brotin, T., Meerschaut, D., Clavier, G., Placin, F., Pozzo, J. L., and Bouas-Laurent, H. (2004) *New. J. Chem*., 28:234–243.
7. Rajamalli, P., and Prasad, E. (2011) *New J. Chem*., 35:1541–1548.
8. George, S. J., and Ajayaghosh, A. (2005) *Chem. Eur. J*., 11:3217–3227.
9. Ajayaghosh, A., Chithra, P., and Varghese, R. (2007) *Angew. Chem., Int. Ed.*, 46:230–233.
10. Zhang, X., Chen, Z., and Wurthner, F. (2007) *J. Am. Chem. Soc*., 129:4886–4887.
11. Boerakker, M. J., Botterhuis, N. E., Bomans, P. H. H., Frederik, P. M., Meijer, E. M., Nolte, R. J. M., and Sommerdijk, N. A. J. M. (2006) *Chem. Eur. J*., 12:6071–6080.
12. Qu, S. N., Chen, X. F., Shao, X., Li, F., Zhang, H. Y., Wang, H. T., Zhang, P., Yu, Z. X., Wu, K., Wang, Y., and Li, M. (2008) *J. Mater. Chem*., 18:3954–3964.
13. Qu, S. N., and Li, M. (2007) *Tetrahedron*, 63:12429–12436.
14. Shirakawa, M., Fujita, N., Tani, T., Kaneko, K., and Shinkai, S. (2005) *Chem. Commun*., 4149–4151.
15. Vemula, P. K., Li, J., and John, G. (2006) *J. Am. Chem. Soc*., 22:775–779.
16. Eastoe, J., Sanchez-Dominguez, M., Wyatt, P., and Heenan, R. K. (2004) *Chem. Commun*., 2608–2609.
17. Yagai, S., Nakajima, T., Kishikawa, K., Kohmoto, S., Karatsu, T., and Kitamura, A. (2005) *J. Am. Chem. Soc*., 127:11134–11139.
18. Sugiyasu, K., Fujita, N., Takeuchi, M., Yamada, S., and Shinkai, S. (2003) *Org. Biomol. Chem*., 1:895–899.
19. Thomas III, S. W., Joly, G. D., and Swager, (2007) T. M. *Chem. Rev*., 107:1339–1386.
20. Grell, M., Bradley, D. D. C., Ungar, G., Hill, J., and Whitehead, K. S. (1999) *Macromolecules*, 32:5810–5817.
21. Shinto, V., Nambalan, S., Saleesh, K., Anjali, K., Doddamane, S., Shankar, R., Subbarao, K. P., and Suresh, D. (2009) *Adv. Funct. Mater*, 19:2064–2073.
22. Birks, J. B. (1970) *Photophysics of Aromatic Molecules*. Wiley: London.
23. Xie, Z. Q., Xie, W. J., Li, F., Liu, L. L., Wang, H. A., and Ma, Y. G. (2008) *J. Phys. Chem. C*, 112:9066–9071.
24. Ziessel, R., Pickaert, G., Camerel, F., Donnio, B., Guillon, D., Cesario, M., and Prange, T. (2004) *J. Am. Chem. Soc*., 126:12403–12413.
25. Camerel, F., Bonardi, L., Schmutz, M., and Ziessel, R. (2006) *J. Am. Chem. Soc*., 128:4548–4549.
26. Hong, Y. N., Lam, J. W. Y., and Tang, B. Z. (2009) *Chem*. Commun., 4332–4353.
27. Pham, Q. N., Brosse, N., Frochot, C., Dumas, D., Hocqueta, A., and Jamart-Grégoire, B. (2008) *New J. Chem*., 32:1131–1139.
28. Qu, S. N., Zhao, L. J., Xiu, Z.Y., and Li, M. (2009) *Langmuir*, 25:1713–1717.
29. Zhang, P., Wang, H. T., Liu, H. M., and Li, M. (2010) *Langmuir*, 26:10183–10190.
30. Luboradzki, R., Gronwald, O., Ikeda, A., and Shinkai, S. (2000) *Chem. Lett.*, 29:1148–1149.
31. Babu, S. S., Praveen, V. K., Prasanthkumar, S., and Ajayaghosh, A. (2008) *Chem. Eur. J.*, 14:9577–9584.
32. Abdallah, D. j., and Weiss, R.. G. (2000) *Langmuir*, 16: 352–355.
33. Skrovanek, D. J., Howe, S. E., Painter, P. C., and Coleman, M. M. (1985) *Macromolecules*, 18:1676–1683.
34. Harris, P. I., and Chapman, D. (1995) *Biopolymers*, 37:251–263.
35. Ran, X., Zhang, P., Qu, S. N., Wang, H. T., Bai, B. L., Liu, H. M., Zhao, C. X., and Li, M. (2011) *Langmuir*, 27:3945–3951.
36. Wang, H. T., Bai, F. Q., Liu, H. M., Bai, B. L., Ran, X., Qu, S. N., Shi, J.H., Xie, D. J., Li, H. Y., Li, M., and Zhang, H. X., (2011) *Phys. Chem. Chem. Phys*., 13:9697–9705.
37. Winnik, F. M. (1993) *Chem. Rev*., 93:587.
38. Zagrobelny, J., Betts, T. A., and Bright, F. V. (1992) *J. Am. Chem. Soc*., 114:5249–5257.
39. Kane, M. A., Baker, G. A., Pandey, S., Maziarz III, E. P., Hoth, D. C., and Bright, F. V. (2000) *J. Phys. Chem. B*., 104:8585–8591.
40. Lu, L. D., Helgeson, R., Jones, R. M., Mcbranch, D., Whitten, D. (2002) *J. Am. Chem. Soc*., 24:483–488.
41. Lindsay, G. A., Hollins, R. A., Zarras, P., Guenthner, A. J., Chafin, A. P., Davis, M. C., Fallis, Stephen. U.S. Pat. (2003) *Appl. Publ*. 11 pp.
42. Freydank, A., Janietz, S., and Schulz, B. (1998) *Journal of Electroanalytical Chemistry*, 456:61–69.
43. Terazzi, E., Torelli, S., Bernardinelli, G., Rivera, J. P., Benech, J. M., Bourgogne, C., Donnio, B., Guillon, D., Imbert, D., Bunzli, J. C. G., Pinto, A., Jeannerat, D., and Piguet, C. (2005) *J. Am. Chem. Soc*., 127:888–903.
44. Zhang, Y. D., Jespersen, K. G., Kempe, M., Kornfield, J. A., Barlow, S., Kippelen, B., and Marder, S. R. (2003) *Langmuir*, 19:6534–6536.
45. Dave, J. S., and Vora, R. A. (1970) Liquid Crystals and Ordered Fluids; Plenum: New York, 477.